Journal of The Electrochemical Society

The Electrochemical Society
Advancing solid state & electrochemical science & technology

OPEN ACCESS

Calcination Temperature Dependent Catalytic Activity and Stability of IrO_2 –Ta_2O_5 Anodes for Oxygen Evolution Reaction in Aqueous Sulfate Electrolytes

To cite this article: W. Xu *et al* 2017 *J. Electrochem. Soc.* **164** F895

View the article online for updates and enhancements.

This content was downloaded from IP address 78.91.96.174 on 05/10/2020 at 11:10

Calcination Temperature Dependent Catalytic Activity and Stability of IrO_2 –Ta_2O_5 Anodes for Oxygen Evolution Reaction in Aqueous Sulfate Electrolytes

W. Xu,[a,*,z] G. M. Haarberg,[a,] S. Sunde,[a] F. Seland,[a,**] A. P. Ratvik,[b] E. Zimmerman,[c] T. Shimamune,[c,**] J. Gustavsson,[c,**] and T. Åkre[d]**

[a]*Department of Materials Science and Engineering, Norwegian University of Science and Technology, NO-7491 Trondheim, Norway*
[b]*SINTEF Materials and Chemistry, NO-7491 Trondheim, Norway*
[c]*Permascand AB, SE-84010 Ljungaverk SE, Sweden*
[d]*Glencore Nikkelverk AS, NO-4613 Kristiansand S, Norway*

In this work, commercial IrO_2-Ta_2O_5 anodes with a certain composition calcined at three different temperatures were investigated. The results show that the calcination temperature has a significant influence on the electrocatalytic activity for the oxygen evolution reaction (OER). This is attributed to the influence of the calcination temperature on the surface microstructure including the crystallinity and the preferred orientation of IrO_2 crystallites of the IrO_2-Ta_2O_5 binary oxide formed. The surface morphology of the anodes was revealed as mud-cracks surrounded by flat areas containing several scattered IrO_2 nanocrystallites. The size of these nanocrystallites, which in turn contribute to the electrochemical active surface area, is dependent on calcination temperature. The (101)-surfaces of the IrO_2 were found to have higher catalytic activity than (110) IrO_2 with respect to the OER. The (101) IrO_2 planes were dominating at low or moderate calcination temperatures, whereas the (110) IrO_2 orientation was preferred at the highest calcination temperature. Accelerated lifetime tests of the investigated samples indicate that the (101) IrO_2 is more stable (110) IrO_2 during electrolysis. A moderate temperature is suggested as the best calcination temperature for this type of anode regarding the electrochemical active surface area, electrocatalytic activity and stability for OER in acidic aqueous electrolytes at operating conditions.

© The Author(s) 2017. Published by ECS. This is an open access article distributed under the terms of the Creative Commons Attribution 4.0 License (CC BY, http://creativecommons.org/licenses/by/4.0/), which permits unrestricted reuse of the work in any medium, provided the original work is properly cited. [DOI: 10.1149/2.0061710jes] All rights reserved.

Manuscript submitted April 26, 2017; revised manuscript received June 8, 2017. Published June 22, 2017. This was Paper 1653 presented at the Honolulu, Hawaii, Meeting of the Society, October 2–7, 2016.

Efficient electrowinning (EW) in aqueous sulfate electrolytes depends on fast reaction kinetics, low ohmic resistances and suppression of parasitic and detrimental reactions. The overall cell voltage is determined by the thermodynamic potentials for metal deposition (cathode) and oxygen evolution (anode), in addition to overpotentials and ohmic voltage drops. The sluggish reaction kinetics of the oxygen evolution reaction (OER) in low-pH sulfate electrolytes lead to rather high anode overpotential at industrial relevant current densities, thus being a significant contributor to an increased cell voltage.[1] The low pH, moderate temperature and high anode potential in aqueous metal electrowinning limit the anode material selection significantly, as few materials are stable at these operating conditions. Therefore, identifying an efficient anode catalyst to facilitate the OER by lowering the overpotential has been considered an important research field over many decades also in copper EW.[2,3] From an industrial perspective, stability and service lifetime of the anodes are just as important as the electrocatalytic activity. Ru oxide catalysts are known to be the most active for OER,[4] but not stable enough for long term operation in the acidic environment.[5] IrO_2 is also very active toward OER and significantly more stable than RuO_2, but also suffers from some degradation during prolonged operation.[6–9] Comninellis and Vercesi performed a comprehensive study of nine different binary catalyst coatings.[10] They reported that the 70 mol% IrO_2 – 30 mol% Ta_2O_5 catalyst coating on Ti substrate gave by far the best electrocatalytic activity toward the OER. A similar optimum composition has later been reported by Krýsa et al.,[11] Xu and Scantlebury,[12] and Vercesi et al.[13] Thus, the industrial OER catalyst benchmark today is comprised of an oxide mixture of IrO_2 (ca 70 mol%) and Ta_2O_5 (ca 30 mol%), where both catalytic activity and stability are considered. These oxide catalysts are deposited onto pretreated titanium substrate and commonly referred to as dimensionally stable anodes (DSA).[4]

Although the promoting catalytic effect of adding inert Ta_2O_5 oxide to the IrO_2 catalyst is not well understood, it is clear that the electrocatalytic properties of the anode depend significantly on the catalysts microstructure, such as surface morphology and phase composition.[7,11,12,14] A larger electrochemically active surface area (ECSA) will also provide more sites for oxygen evolution and thus lead to a lower operating voltage. Xu and Scantlebury[12] concluded that the anodes with 50–70 mol% IrO_2 have not only the largest ECSA, but also the highest electrochemical activity. Also, the 70 mol% IrO_2 with 30 mol% Ta_2O_5 was the best with respect to anode stability. Normally the prepared IrO_2-Ta_2O_5 has a heterogeneous "mud-crack" surface morphology, which is surrounded by a flat area with dispersed IrO_2 and IrO_2 aggregates.[14] The boundaries of IrO_2 crystallites are modified by amorphous Ta_2O_5. Otogawa and co-workers[14] concluded that the fine IrO_2 particles (around 30–100 nm) on the flat area in the coating surface dominate as catalyst for OER while the others such as the larger IrO_2 aggregates and the IrO_2 particles embedded in the cracks show little influence. Our group[15] has reported that even smaller IrO_2 particles of 10 nm or less, which are uniformly dispersed on the "flat area" of the coating, have very good catalytic activity for OER. However, the impact of IrO_2 crystallites size in this binary oxide on the catalytic activity toward OER is still not clear.

As mentioned above, lifetime is another issue for anodes in industrial applications. Martelli and co-workers[16] demonstrated that the deactivation mechanisms of IrO_2-Ta_2O_5/Ti anode can generally be attributed to the consumption of the active component in the coating layer and/or the passivation of the substrate beneath the coating layer, which mainly depends on the coating microstructure. Furthermore, it has been proposed that the deactivation process of the anode is as follows: (1) the dissolution of coated oxides as the dominating stage, i. e. IrO_2 loss from preferential orientations of (110) and (101), (2) dissolution and anodic oxidation of the Ti substrate, which then leads to coating detachment and failure of the anode.[17,18] Based on basic thermodynamic considerations, metal oxides always become unstable under OER conditions, irrespective of the pH.[19] This implies that, the lifetime of an oxide anode under OER will always be

*Electrochemical Society Student Member.
**Electrochemical Society Member.
[z]E-mail: xiaohui916@gmail.com

limited. Consequently, enhancing the stability of the coating layer to impede the dissolution process is as important as improving the electrocatalytic activity toward OER through modification of the coating microstructure.

The IrO_2-Ta_2O_5/Ti anodes are usually prepared by thermal decomposition of a precursor containing iridium and tantalum salts. The pretreatment of the substrate and the thermal decomposition processes influence the properties of the anode as well as the final coating composition. The thermal decomposition condition is one parameter which significantly influences the microstructure and catalytic properties of the IrO_2-Ta_2O_5/Ti anode. In order to find an optimum anode preparation procedure, the effect of calcination temperature, precursor solvent, coating thickness, ternary (or more) oxide mixtures, coating techniques, and pretreatment of the titanium substrate have been investigated.[11,20–24] Most of the studies investigated the microstructure and electrochemical performance of the IrO_2-Ta_2O_5 anode through a variation of the Ir: Ta ratio as well as the calcination temperature.[10,12,13] The best Ir-Ta-O coating layer is suggested to have a molar Ir content of 65–70%. In spite of many efforts, the effect of preparation condition, such as calcination temperature, on catalytic activity and durability is not fully understood.

In this work, IrO_2 - Ta_2O_5 type anodes with 70–80 mol% Ir for industrial use have been calcined at three different temperatures within a range representative for industrial coatings, where a mix of amorphous and crystalline catalyst material is obtained. An investigation of the effect of calcination temperature on microstructure, coating properties, catalytic activity and lifetime has been performed. In particular, surface morphology and coating properties, such as crystallite orientation have been investigated. We show that the catalyst activity toward OER depends strongly on the calcination temperature and hence the microstructure of the catalyst layer. A trend of calcination temperature dependence of preferable rutile IrO_2 orientation for this type of anode is demonstrated. Combined with lifetime predictions, the relationship between calcination temperature and durability of the anodes is also discussed.

Experimental

Anode preparation.—IrO_2-Ta_2O_5 coated titanium samples were prepared by Permascand AB of Sweden. First, the titanium substrates were etched in 2% hydrofluoric acid to remove most of the less conductive titanium oxides and to obtain a proper roughness of the surface prior to coating. Next, a thin interlayer was prepared on the pretreated titanium substrate to improve adhesion and impede underlying titanium oxide formation. Finally, in-house prepared precursor films were applied to the coated Ti substrate by a brush coating technique and dried. In order to evaporate the solvent in the precursor film, the brushed samples were dried at room temperature then sintered at a fixed temperature[e] in the range from 400–550°C in ambient air for about 10–20 minutes. The brushing, drying and sintering procedure was repeated several times until the targeted loading of Ir amount was obtained. In this work, three different temperatures were applied for the calcination, denoted as 'low T', 'moderate T', and 'high T', respectively.

Microstructure measurements.—Surface morphology and chemical composition of the DSA samples were analyzed using scanning electron microscopy (SEM, Zeiss Supra) combined with energy dispersive spectroscopy (EDS). X-ray diffraction (XRD) studies were carried out directly on the surface of anode samples using Bruker AXS D8Advance with Cu Kα radiation. Data were collected by varying the 2θ angle from 10° to 80° with an increment of 0.02°. The crystalline structure, physical phase and texture of the coating of the DSA samples were calculated by fitting of XRD patterns with X'Pert HighScore Plus.

[e]The exact calcination temperatures are confidential information.

Electrochemical studies.—The electrochemical behavior of the commercial anode samples was characterized by cyclic voltammetry (CV) and potentiodynamic polarization measurements to determine ECSA and electrocatalytic activity. The electrochemical experiments were carried out in a classical three electrode system using a Gamry REF600 potentiostat. A DSA electrode fixed in a Teflon sample holder exposing 1 cm^2 of the electrode area was used as the working electrode. A Pt mesh was used as the counter electrode, while a reversible hydrogen electrode, placed in the working electrode electrolyte compartment was used as the reference electrode. All experiments were conducted in 0.9 M H_2SO_4 aqueous electrolyte at 60°C in a temperature controlled water bath. Before each experiment, the electrolyte was deaerated with purified argon (Yara, 5.0) gas purging for a few minutes. Cyclic voltammetry measurements were recorded between 0.15 V and 1.4 V vs. RHE for sweep rates from 5 to 500 mV/s. Polarization measurements were conducted from 1.4 V at a sweep rate 5 mV/min in order to approach steady state. The IR drop was corrected by using the measured electrolyte resistance taken as high frequency real axis intersection of the electrochemical impedance spectra. Electrochemical impedance spectroscopy (EIS) was performed at various dc potentials with a peak to peak ac amplitude of 10 mV/rms from 0.01 Hz to 100 kHz and with 10 points per decade.

To obtain reproducible electrochemical measurements, some pretreatment of the anodes was found to be necessary as the porous coating combined with destructive gas evolution could lead to large changes in the active surface area with time.[6] Preconditioning the anodes with 200 potential cycles at 100 mV/s was found to give satisfying reproducibility and was thus run on all anode samples before recording the reported E-I curves. This preconditioning must be distinguished from the stabilization stage during operation of an industrial electrolysis cell.

Lifetime studies.—Considering the lifetime of this type of anode could be several years, accelerated lifetime tests were carried out to reveal the durability of those anodes. The lifetime tests were performed under galvanostatic conditions in acidic 0.9 mol/L Na_2SO_4 solution at a current density of 5 kA/m^2. The temperature was maintained at 60°C by using heating elements in the electrolyte. The potential of the tested electrode was monitored. The electrode was considered to be deactivated when the cell voltage reached 10 V. The lifetime was then recorded as the time until deactivation. The Ir losses of the coatings during the test were measured by X-ray fluorescence (XRF).

Results and Discussion

XRD measurements and surface morphology.—Figure 1 shows the XRD pattern of the IrO_2-Ta_2O_5 electrode as a function of the calcination temperature. In all samples investigated we observed well-defined peaks corresponding to the IrO_2 rutile phase and to Ti metal, while no peaks corresponding to Ta_2O_5 phase were observed. We thus assume the latter be present as an amorphous phase. Diffraction peaks corresponding to three different Miller indexes of IrO_2 were detected in the investigated samples, viz. (110), (101), (211) and (200). The (211)-peak was only observed for the two samples annealed at the highest temperature. As the peaks are getting sharper with increasing calcination temperature, we infer from Figure 1 an increased order, i. e. the degree of crystallinity increase, with increasing calcination temperature as expected in Ref. 25 However, the coating layer may not be fully oxidized since the calcination temperatures are all lower than 600°C.[25] For the sample calcined at the lowest temperature very broad IrO_2 peaks, and in this case the (211)-peak is not visible at all. This indicates the formation of a substantially less ordered IrO_2 or even amorphous catalyst at low calcination temperatures.

d-spacing values were calculated by fitting the XRD patterns and listed in Table I together with estimated average crystallite sizes. The crystallite sizes of IrO_2 were roughly estimated based on full width at half maximum (FWHM) combined by using the Scherrer Equation,

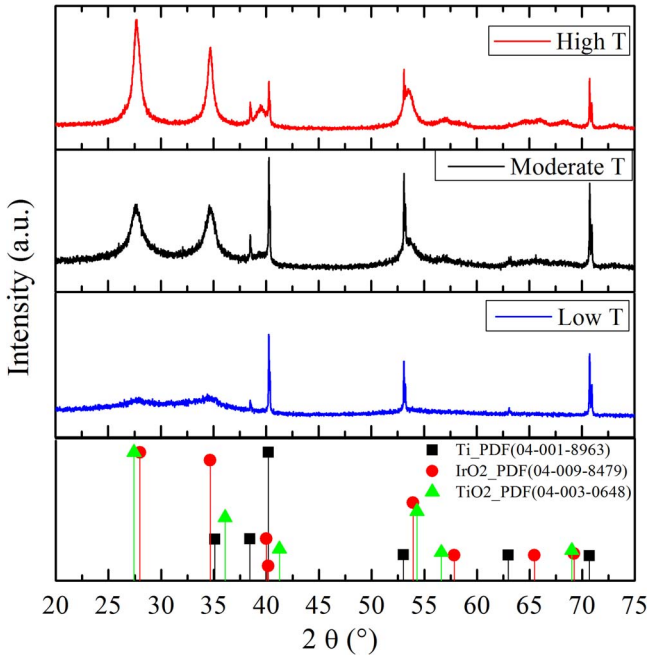

Figure 1. XRD patterns of the IrO_2-Ta_2O_5 electrode s calcined at three different temperatures. (The lower pane displays the standard PDF of Ti metal, rutile IrO_2 and Rutile TiO_2).

as shown in Eq. 1.[26]

$$t = \frac{0.9\lambda}{B\cos\theta_B} \quad [1]$$

where t is the particle size, B is the full width at half maximum, and θ_B is the peak diffraction angle. λ is the wavelaength. From the results in Table I the find that the d-spacing of the samples investigated here are consistently larger than those of pure IrO_2 (powder sample). Also, Table I shows that increasing the calcination temperature leads to a moderate increase in particle size. The increase in d-spacing values in all observed facets can be explained in terms of $Ir(Ta)O_2$ solid solution formation in the presence of tantalum, as a result of the interaction between the rutile structure of both Ir and Ta oxides. Furthermore, all these chemical reactions take place on titanium substrate which would induce lattice strain into the formed coating layer.

Apparently (101) IrO_2 crystallites formed at moderate temperature might be less stressed and/or less influenced by dissolved Ta atoms. Meanwhile the d-spacing of (110) IrO_2 crystallites formed at moderate temperature became larger. Due to lack of knowledge about the specific solid solution, we cannot draw clear-cut conclusions whether Ta would be placed at interstitial or substitutional positions. Considering that the atom radius difference between Ir and Ta is very small, it makes the substitutional replacement much easier to happen.[27] Thus, we believe that the dissolved Ta is more likely to be placed substitutional than interstitial. Formation of partial interstitial solid solution is expected to be possible as the existence of defects in this binary oxide compound is common as well as being not fully oxidized while electroneutral has been considered.

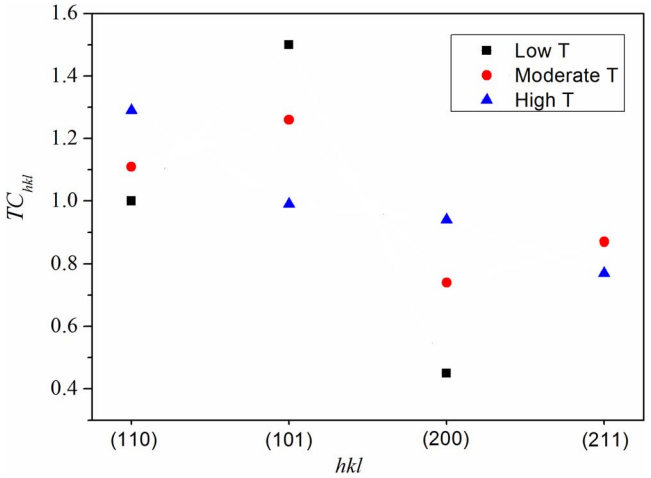

Figure 2. Estimated texture coefficients ($TC_{(hkl)}$) for IrO_2 (Eq. 1) as a function of calcination temperature.

From the estimated average crystallite sizes of IrO_2 in Table I we can see that a high calcination temperature gives the largest crystallites. It seems that similar crystallite sizes of IrO_2 are obtained with "low T" and "moderate T", which indicates that the crystallite size varies with the crystallographic direction. It suggests a preferable orientation during formation of IrO_2 crystals. Preferential facet orientation can be recognized through estimation of texture coefficients (TC(hkl)) of IrO_2 (Eq. 1).[28] Calculated texture coefficients are presented in Fig. 2.

$$TC_{(hkl)} = \frac{I_{(hkl)}/I_{0(hkl)}}{\frac{1}{n}\sum_{1}^{n} I_{(hkl)}/I_{0_{(hkl)}}} \quad [2]$$

where $I_{(hkl)}$ is the measured intensity of the *(hkl)* plane, $I_{0(hkl)}$ is the standard intensity of the standard XRD patterns data, and n is the total number of reflections. It should be mentioned that, according to the theory of texture coefficients, Eq. 2, only values of TC greater than one can be considered as having texture.

Our results indicate that (110) is the preferred as grown orientation of IrO_2 when a high calcination temperature is used, c.f. Fig. 2. This is in correspondence with the results reported by Hu et al.[29] However, at low calcination temperature we found that the (101) IrO_2 orientation is preferred. According to Hu et al., the (101) rutile IrO_2 displays better catalytic activity since the length of the bond for Ir-O is shorter for (101) than for other facets.[29] (101) IrO_2 formed at moderate temperature, in our case, could have shorter Ir-O bond since the d-spacing is smaller, which could also affect catalytic activity.

Figure 3 depicts the surface morphology of IrO_2-Ta_2O_5 coatings calcined at different temperatures. All coatings display cracks surrounded by smooth, relatively flat areas. On a larger scale the crack structures appear more or less similar from sample to sample. However, the internal morphology of the cracks is different as can be seen in the higher-magnification images to the right in Figure 3. The latter

Table I. d-spacing value and estimated average crystallite size.

	d-spacing / Å				Average crystallite size / nm		
hkl	IrO2 PDF	Low T	Moderate T	High T	Low T	Moderate T	High T
110	3.185	3.208	3.223	3.219	8.8	6.3	10.0
101	2.568	2.592	2.582	2.586	6.3	8.0	12.6
200	2.253	2.269	2.274	2.276	2.3	6.9	6.9
211	1.699	-	1.709	1.711	-	8.6	9.7

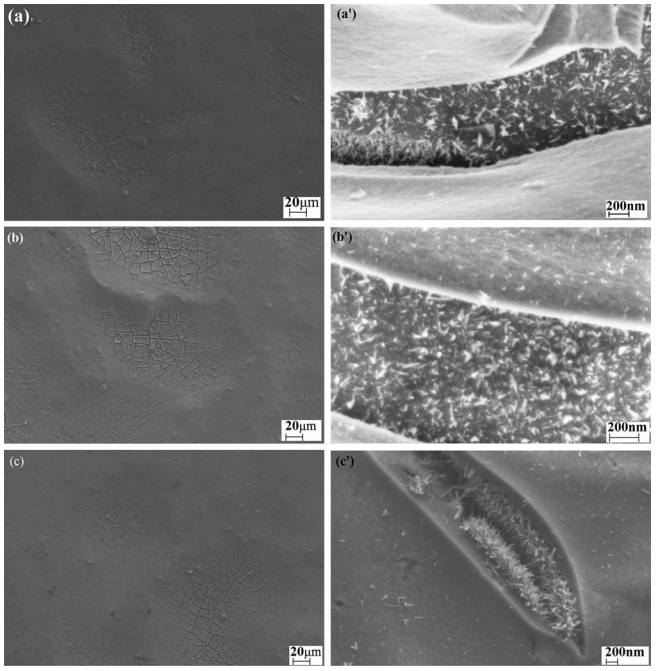

Figure 3. SEM images of IrO_2-Ta_2O_5/Ti anode (a) & (a′) calcined at low temperature, (b) & (b′) calcined at moderate temperature, (c) & (c′) calcined at high temperature.

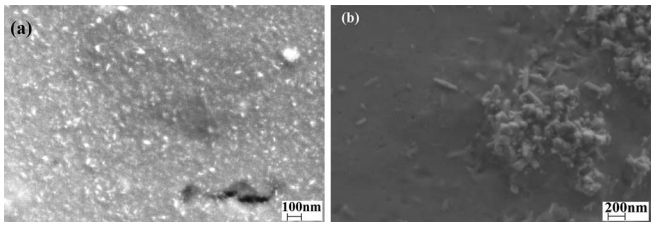

Figure 4. SEM images of selected regions of the "flat area" of the calcined anodes, (a) calcined at moderate temperature, (b) calcined at high temperature.

indicate that dense needle-like nano-scale crystallites have formed inside cracks during sintering. EDX analysis shows that the needle-like particles enriched in iridium, and thus nano crystallites of IrO_2 appear to grow inside cracks. A few IrO_2 nano particles were observed on the neighboring flatter areas outside the cracks for the samples calcined at the higher temperatures, but was barely observed on samples calcined at low temperature since the coating calcined at the low temperature is partially amorphous, as shown in Fig. 4. All these nano crystallites grow bigger with increasing calcination temperature. As a result, apparent ball-shaped nano crystallites were formed in the flat area at moderate temperature while nano cylinders were formed as aggregates at high temperature.

IrO_2 formation is a crystallization process preceded by nucleation during thermal decomposition, which always takes place in a site having a higher Gibbs free energy. Hence, the crystallization may be heterogeneous and cause the surface to form with a different morphological constituent. It is interesting to note the correlation between the structure coefficients and the development of the texture coefficients in Figure 2 and the morphology development in Figure 3. However, as the balance of the structure may also depend on calcination temperature an unequivocal conclusion in terms of the structure of the surface deposits in isolation is not possible.

Catalytic activity.—The voltammetric behavior observed for the calcined anodes is typical for thermally prepared oxide coatings, as shown in Figure 5a. The displayed broad peaks between the OER and the hydrogen evolution correspond to oxidation state transitions of noble metals (Ir^{3+}/Ir^{4+} in this case).[30] It is clear that the peak current decreases with increasing calcination temperature and moves the onset potential of OER toward more positive potentials. Since the oxide compositions are almost equal, an apparent change in voltammetric response and OER onset potential may be attributed to the surface morphology and a change in active surface area. The ECSA of these anodes are estimated by extrapolating the voltammetric charge q∗ to infinite sweep rates, i.e. when only outer charge is probed. The charge is measured from integration of the current vs time curves equivalent to a potential scan between 0.15 and 1.4 V. The total charge q∗ can conceptually be split into an inner and an outer charge, according to the following equation:[10]

$$q^* = q_{\text{inner}} + q_{\text{outer}} \quad [3]$$

where the q_{inner} and q_{outer} are the charges related to the "inner" and the "outer" surface, respectively. The inner surface is the less accessible parts of the surface such as pores, cracks, defects, grain boundaries and etc., whereas the outer surface relates to the more accessible parts of the surface to the electrolyte. They also offer an approach to obtain the charge values by extrapolation both at $v = 0 (q^*)$ and at $v = \infty (q_{outer})$, where v is the sweep rate.

As shown in Figure 5b, the maximum values for all charges are obtained with the coating calcined at the low temperature. The ECSA of the coating calcined at "low T" is about twice as large as that at "moderate T" and five times larger than the one at "high T". This

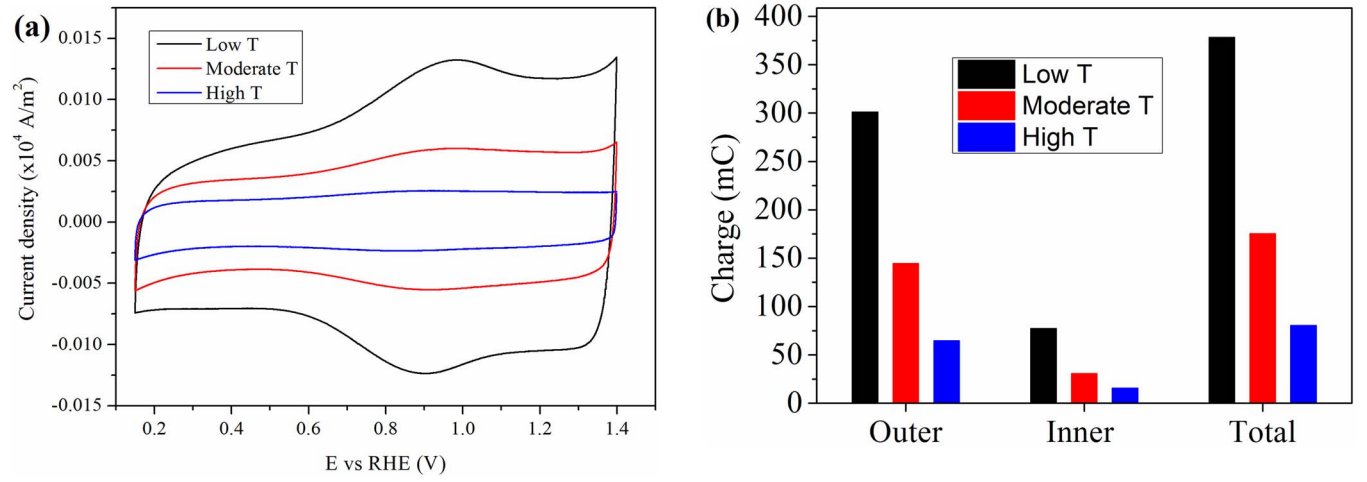

Figure 5. (a) Cyclic voltammetry of calcined anodes at different temperatures, (b) Voltammetric charge calculated by integration and extrapolating of CV curves.

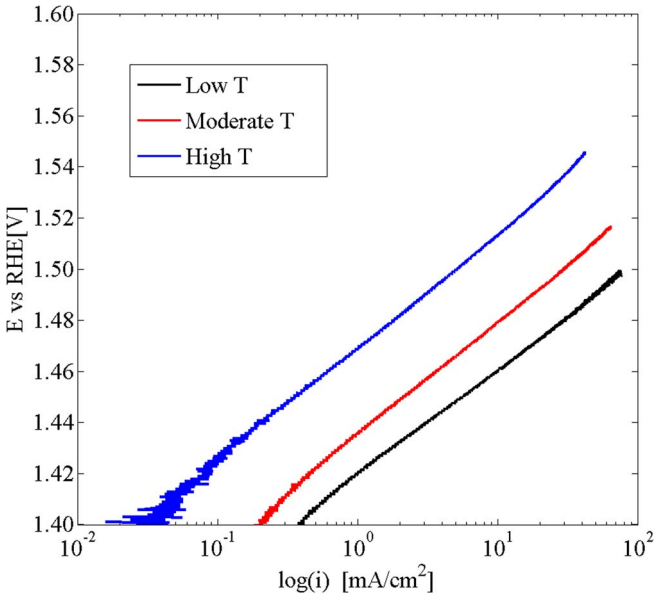

Figure 6. IR compensated polarization curves of different anodes, scan rate 5 mV/min.

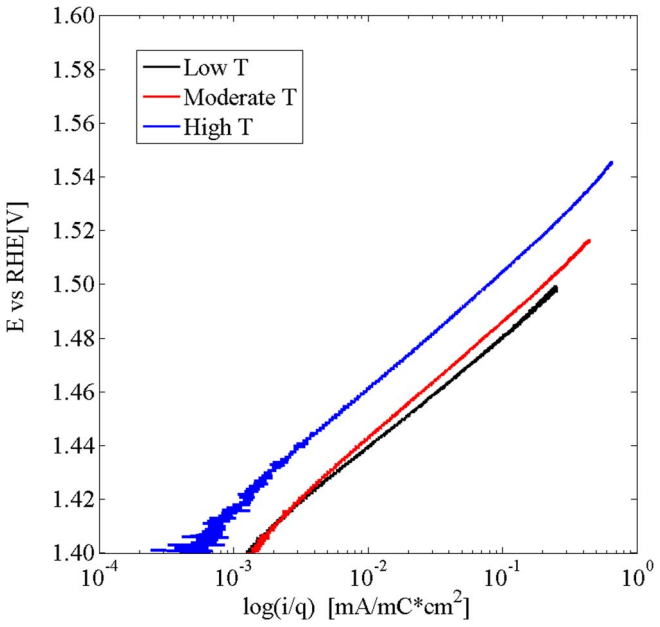

Figure 7. Normalized polarization curves on anodes calcined at different temperatures with respect to outer charge, which gives a measure of the electrocatalytic activity per unit active surface area.

indicates that the ECSA decreases with increasing the calcination temperature of the anode, and thus implies that the number of active sites on the coating decrease with higher calcining temperature. Moreover, the ECSA is significantly affected by the surface morphology as expected. The results indicate that:

(1) Active sites on the anode surface are determined by the fine IrO_2 crystallites. The more and finer the IrO_2 crystallites are, the more active sites are contributing.
(2) The amorphous parts of the IrO_2 may contribute more that the crystalline parts of the electrode through a larger number of active sites on the surface due to the disorder of the amorphous oxide.

The IR-corrected polarization curves obtained for all anodes are shown in Figure 6. Coating of "low T" shows the best activity as a result of holding the largest ECSA. In comparison the "high T" is the electrode with the lowest activity. Similar results have been found on IrO_2/Ti anode by Trasatti,[4] where it was concluded that the electrocatalytic activity of the OER increases with decreasing calcining temperature in the range from 350–550°C. Apparently the activity for the OER of this type of anode is calcining temperature dependent, which is determined by the amount of active sites. An interesting relationship between current density and ECSA has occasionally been found, showing a square interrelationship between current density and ECSA for the examined anodes. As an example, at potential of 1.45V vs RHE, the current density for "low T" is about 4 times higher than that for "moderate T" and 25 times higher than that for "high T."

In order to compare the catalytic activity difference per unit active area among the samples, the polarization curves have been normalized with respect to the outer charge, as shown in Figure 7. Here we can see the "low T" anode still holds the best activity, which is approximately 30 times higher than that of "high T" anode with respect to current density. The "moderate T" anode is almost as good as the "low T" anode. This means that the comparable catalytic activity and active sites between these two samples are almost equivalent. The slight difference is believed to be due to the formation of partial amorphous IrO_2 in "low T" coating. Amorphous IrO_2 has higher reactivity than crystalline IrO_2 as concluded by Thanawala et al.,[31] which also has been reported by Morimitsu et al.[20] Yet in this case it is most likely that the IrO_2 nanocrystallites nested inside cracks contribute more to the activity than amorphous IrO_2. Taking into account the preferred orientation of IrO_2 crystallites as function of calcination temperature, it can be concluded that the (101) IrO_2 in this binary oxides has higher catalytic activity for OER than that of (110) IrO_2. Furthermore, the Tafel slopes of all anodes within industrial operational potential range are similar and approximately 45 mV/decade. Hence, the Tafel slope is independent of calcination temperature. The slight difference is attributed to the existence of the partial amorphous phase.

Durability.—Figure 8 shows the results of the measurement of accelerated lifetime tests on the anodes calcined at different temperatures. The lifetime is approximately 4500 hours for the "low T" sample. Although it holds the best catalytic activity, the lifetime is much shorter than the others. This could be attributed to the poor crystallinity of IrO_2 in the coating as low crystallinity implies less stability and high dissolution. Lifetimes of the other two electrodes are more than 10000 hours. It should be added that we got counter electrode failure while running the lifetime test about 11000 hours, thereby the practical lifetime of the samples calcined at "moderate T" and "high T" could be even longer under the testing condition in this case. Thus, in this case it is not possible to predict which one has the longer lifetime of the "moderate T" and "high T". However, it can be

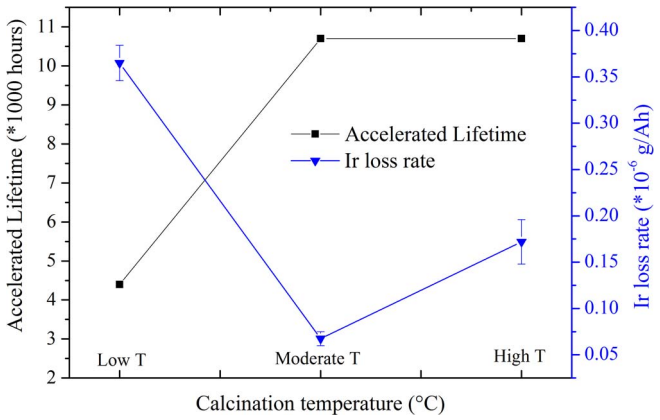

Figure 8. Lifetime of the IrO_2-Ta_2O_5 anode calcined at different temperature (black square), and Ir loss rate during accelerated lifetime tests (blue triangle).

assumed that the longest lifetime is obtained for "moderate T" based the lower Ir loss rate (blue spots in Figure 8) compared to "high T". Regarding the Ir loss during long time electrolysis, more Ir loss means less effective active component left in the coating overtime. The cell potential then increases to maintain the applied current density. The electrode would be deactivated when reaching a high potential due to reduced amount of Ir on the electrode as the active component in the coating can no longer support the OER. For instance the "low T" sample is only lasting approximately 4500 hours combined with quite high Ir loss rate.

Considering the catalyst properties discussed in the first section, and as a result of the variation of calcination temperature, the preferred orientation of IrO_2 impacts not only the morphologies but also the catalytic activity. The results of lifetime tests confirm experimentally that the (101) IrO_2 has higher stability than (110) IrO_2 since the sample with (101) preferred orientation has the longest lifetime. Although it has been reported experimentally that the stability of (101) IrO_2 crystallites for OER is better than (110) IrO_2,[17] it is less evident from our results. This is because in that case the conclusion was given by measuring the TC(hkl) values of both the (101) and (110) IrO_2 which decrease over time. However, there is no remarkable difference between those two values if the experimental error is taken into account. Obviously, compared to (110) IrO_2, (101) IrO_2 supplies higher catalytic activity for OER and resistance to corrosion in acidic solution. This could be attributed to the fact that the (101) plane is one of the most close-packed planes of the IrO_2 rutile phase.[32] Therefore, coatings with preferred (101) IrO_2 show the best results both on catalytic activity and stability for the oxygen evolving anode in acidic solutions.

Conclusions

The dependence of calcination temperature for DSA with a commercial IrO_2 - Ta_2O_5 coating was investigated. Three different calcination temperatures were applied in terms of low, moderate and high temperature. The oxide coatings show typical mud-cracks surrounded by a "flat area" as the main feature of surface morphology. A nano crystalline IrO_2 structure was formed both within the cracks and on the "flat area" in all coatings after calcination. The crystallinity and crystallite size of IrO_2 are calcination temperature dependent, and were found to increase with calcination temperature. As a result the IrO_2 nanoparticles formed in the "flat area" aggregates when calcined at high temperature. At low calcination temperature, the coating was not fully decomposed. Almost no IrO_2 nanoparticles are generated on that "flat area", thus the "flat area" is dominated by an amorphous coating. Since the IrO_2 crystals contribute and dominate the amount of active sites, which represents the ECSA, amorphous IrO_2 presents more active sites than the IrO_2 crystalline structure. Additionally, the coatings calcined at low or moderate temperature show preferred (101) planes of IrO_2 crystallites, whereas the ones calcined at high temperature have mostly (110) orientation. It indicates that the nano-IrO_2 crystals as IrO_2 aggregates are a result of (110) crystallites, whereas the (101) crystallites are formed as ball-shaped finer nanoparticles. Except the ECSA, preferred orientation of IrO_2 also has influence on the catalytic activity for OER. The coating calcined at low temperature has the best catalytic activity for OER, whereas the one calcined at moderate temperature was almost similar. Moreover, it was verified that the (101) IrO_2 has higher stability than (110) IrO_2 on OER in long time electrolysis with acidic aqueous electrolyte. Regarding the accelerated lifetime of all investigated anodes, the moderate temperature is suggested as the best calcination temperature in this specific case.

Acknowledgments

The work was carried out in the project "SUPREME". The financial support from NTNU and the Research Council of Norway are greatly appreciated, and co-financed by the following industrial companies: Hydro Aluminium, Glencore Nikkelverk, Permascand and BOLIDEN Odda. Permission to publish the results is gratefully acknowledged.

References

1. W. C. Cooper, *J. Appl. Electrochem.*, **15**, 789 (1985).
2. G. Eggett and D. Naden, *Hydrometallurgy*, **1**, 123 (1975).
3. S. Trasatti, *Electrochim. Acta*, **45**, 2377 (2000).
4. S. Trasatti, *Electrochim Acta*, **29**,1503 (1984).
5. R. Kötz and S. Stucki, *Electrochim. Acta*, **31**, 1311 (1986).
6. G. N. Martelli, R. Ornelas, and G. Faita, *Electrochim. Acta*, **39**, 1551 (1994).
7. J. M. Hu, H. M. Meng, J. Q. Zhang, and S. N. Cao, *Corro. Sci.*, **44**, 1655 (2002).
8. L. K. Xu and J. D. Scantlebury, *Corro. Sci.*, **45**, 2729 (2003).
9. T. Binninger, R. Mohamed, K. Waltar, E. Fabbri, P. Levecque, R. Kötz, and T. J. Schmidt, *Scientific reports*, **5**, 12167 (2015).
10. C. Comninellis and G. P. Vercesi, *J. Appl. Electrochem.*, **21**, 335 (1991).
11. J. Krýsa, L. Kule, and I. Roušar Mráz, *J. Appl. Electrochem.*, **26**, 999 (1996).
12. L. K. Xu and J. D. Scantlebury, *J. Electrochem. Soci.*, **150**, B254 (2003).
13. G. P. Vercesi, J. Y. Salamin, and CH. Comninellis, *Electrochim. Acta*, **36**, 991 (1991).
14. R. Otogawa, M. Morimitsu, and M. Matsunaga, *Electrochim. Acta*, **44**, 1509 (1998).
15. K. Kawaguchi, G. M. Haarberg, and M. Morimitsu, *ECS Trans*,, **16**, 41 (2009).
16. G. N. Martelli, R. Ornelas, and G. Faita, *Electrochim. Acta*, **39**, 1551 (1994).
17. J. M. Hu, H. M. Meng, J. Q. Zhang, and S. N. Cao, *Corro. Sci.*, **44**, 1655 (2002).
18. L. K. Xu and J. D. Scantlebury, *Corro. Sci.*, **45**, 2729 (2003).
19. T. Binninger, R. Mohamed, K. Waltar, E. Fabbri, P. Levecque, R. Kötz, and T. J. Schmidt, *Scientific reports*, **5**, 12167 (2015).
20. M. Morimitsu, T. Yamaguchi, N. Oshiumi, and T. Zhang, *Proceedings of EMC*, **2011**, 975 (2011).
21. G. P. Vercesi, J. Y. Salamin, and CH. Comninellis, *Electrochim. Acta*, **36**, 991 (1991).
22. C. P. De Pauli and S. Trasatti, *J. Electroanalytical Chem.*, **145**, 538 (2002).
23. J. M. Hu, J. Q. Zhang, and C. N. Cao, *Electrochim. Acta*, **403**, 257 (2003).
24. L. Xu, Y. Xin, and J. Wang, *Electrochim. Acta*, **54**, 1820 (2009).
25. Y. E. Roginskaya and O. V. Morozova, *Electrochim. Acta*, **40**, 817 (1995).
26. B. D. Cullity, *Elements of X-ray diffraction*, Addison-Wesley (1956).
27. A. G. Khachaturyan, *Progress in Mater. Sci.*, **22**, 1 (1978)
28. W. F. Gale and T. C. Owner, *Smithells Metals Reference Book*, p. 422.
29. J. M. Hu, H. M. Meng, J. Q. Zhang, J. X. Wu, D. J. Yang, and C. N. Cao, *J. Mater. Sci. Lett.*, **20**, 1353 (2001).
30. G. R. P. Malpass and A. J. Motheo, *J. Braz. Chem. Soc.*, **14**, 645 (2003).
31. S. S. Thanawala, R. J. Baird, D. G. Georgiev, and G. W. Auner, *Appl. Sur. Sci.*, **254**, 5164 (2008).
32. Z. Yan, Y. Zhao, Z. Zhang, G. Li, H. Li, J. Wang, Z. Feng, M. Tang, X. Yuan, R. Zhang, and Y. Du, *Electrochim. Acta*, **157**, 345 (2015).